Integrated physics package of a chip-scale atomic clock*

Li Shao-Liang(李绍良)[a)b)], Xu Jing(徐 静)[b)], Zhang Zhi-Qiang(张志强)[a)b)], Zhao Lu-Bing(赵璐冰)[a)b)], Long Liang(龙 亮)[a)b)], and Wu Ya-Ming(吴亚明)[a)†]

[a)] *State Key Laboratory of Transducer Technology, Shanghai Institute of Microsystem and Information Technology, Chinese Academy of Sciences, Shanghai* 200050, *China*

[b)] *University of Chinese Academy of Sciences, Beijing* 100049, *China*

(Received 29 August 2013; revised manuscript received 23 December 2013; published online 15 May 2014)

The physics package of a chip-scale atomic clock (CSAC) has been successfully realized by integrating vertical cavity surface emitting laser (VCSEL), neutral density (ND) filter, $\lambda/4$ wave plate, ^{87}Rb vapor cell, photodiode (PD), and magnetic coil into a cuboid metal package with a volume of about 2.8 cm^3. In this physics package, the critical component, ^{87}Rb vapor cell, is batch-fabricated based on MEMS technology and *in-situ* chemical reaction method. Pt heater and thermistors are integrated in the physics package. A PTFE pillar is used to support the optical elements in the physics package, in order to reduce the power dissipation. The optical absorption spectrum of ^{87}Rb D1 line and the microwave frequency correction signal are successfully observed while connecting the package with the servo circuit system. Using the above mentioned packaging solution, a CSAC with short-term frequency stability of about $7 \times 10^{-10}\tau^{-1/2}$ has been successfully achieved, which demonstrates that this physics package would become one promising solution for the CSAC.

Keywords: chip-scale atomic clock (CSAC), physics package, ^{87}Rb vapor cell, coherent population trapping (CPT)

PACS: 43.58.Hp, 32.80.Qk, 32.30.Bv, 85.30.De **DOI:** 10.1088/1674-1056/23/7/074302

1. Introduction

Atomic clocks are the most accurate time and frequency standards, and play important roles in global position system (GPS) navigation and positioning, communication networks, network synchronization, time keeping and transport, some scientific fields, and so on. However, the applications of atomic clock have also been limited because of its volume, power dissipation, and price. The miniaturization of atomic clocks is very meaningful, but challenging. Therefore, chip-scale atomic clock (CSAC) based on MEMS fabrication techniques has rapidly become a compelling research hotspot nowadays. The volume of the traditional microwave-excited atomic clock can hardly be further reduced because the dimension of microwave resonance cavity must be as long as the wavelength of the excitation source. Application of coherent population trapping (CPT) to excite microwave resonances with atoms and the recent advances in alkali vapor cell fabrication using MEMS processes have opened a way to the realization of microfabricated atomic clocks.[1]

The basic working principle of CPT atomic clock is shown in Fig. 1. A coherent bi-chromatic laser beam, which is usually emitted from a local-oscillator-modulated VCSEL, passes through an alkali vapor cell. If the frequency difference of the two components of the bi-chromatic laser is equal to the frequency separation of the ground-state hyperfine splitting of the atoms, the bi-chromatic laser interacts with the three energy level system as shown in Fig. 1, and certain atoms will be coherently coupled together and trapped into the ground state, thus a bright spectral line can be observed through detecting the transmitted optical signal with a photodiode (PD). The signal detected by the PD could be processed by signal processing circuit to get the microwave frequency correction signal which is used to lock the frequency of atomic clock. The atomic clock consists of a physics package and a servo circuit system. All the components of physics package, including VCSEL, neutral density (ND) filter, $\lambda/4$ wave plate, ^{87}Rb vapor cell, PD and magnetic coil, and so on, are hardly integrated in traditional ways. The integration of the physics package can not only reduce the dimensions, but also make it easy to realize the CSAC subsequently by connecting the physics package with servo circuit system. Because there is no need of microwave cavity in the CPT atomic clock, it is easy to employ MEMS technology to realize the fabrication of a physics package of CSAC.

So far, there are many countries interested in developing the CSAC. The USA has conducted most research on the CSAC and realized their commercialization. The National Institute of Standards and Technology (NIST) in the USA firstly realized the fabrication of micromachined cesium vapor cells[2] and vertically integrated physics package.[3–5] The total volume of the packaged device was 0.7 cm^3, its power is required to be 110 mW at an ambient temperature of 25 °C, and the realized short-term frequency instability is $6 \times 10^{-10}\tau^{-1/2}$. Symmetricom, Charles Stark Draper Labora-

*Project supported by the Knowledge Innovation Project of Chinese Academy of Sciences (Grant No. KGCX2-YW-143).

†Corresponding author. E-mail: yamingwu@mail.sim.ac.cn

© 2014 Chinese Physical Society and IOP Publishing Ltd

tory, and Sandia National Laboratories in the USA developed a physics package with suspension structure.[6–8] The total volume is less than 1 cm^3. The power consumption is 30 mW and the short-term frequency instability is $4 \times 10^{-11}\tau^{-1/2}$. Since 2008, some European countries have also launched the MAC-TFC FP7 project together to develop the CSAC. So far, they have reported several methods to realize the microfabrication of alkali atom vapor cell[9–11] which is the heart of the CSAC, yet few physics package were reported. In China, Peking University[12] has succeeded to fabricate ^{85}Rb vapor cell and some other researchers[13,14] reported relevant progress recently.

In this article, we successfully realized the physics package of CSAC by integrating all discrete components into a cheap cuboid metal package. In the physics package, the ^{87}Rb vapor cell has a dual-chamber structure to prevent the impurity generated in reaction from blocking light path, and platinum (Pt) heater and thermistor are integrated on the surface of the vapor cell. In the following sections, the structure and fabrication of ^{87}Rb vapor cell based on MEMS process is described briefly. Then the fabrication of physics package of CSAC is demonstrated in detail, including optical path design, thermal management, and magnetic shielding. At last, the optical absorption spectrum and the microwave frequency correction signal are presented. The total volume of the physics package is about 2.8 cm^3, and it is connected with a servo circuit system to form a CSAC. A short-term frequency stability of about $7 \times 10^{-10}\tau^{-1/2}$ has been measured with the fabricated CSAC.

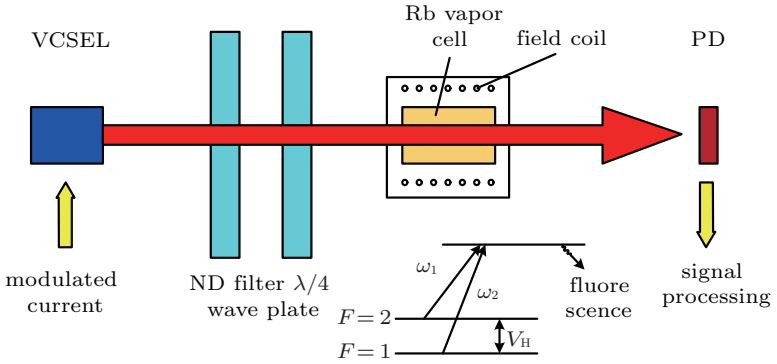


Fig. 1. (color online) Schematic diagram of CPT-based atomic clock working principle.

2. Microfabrication of the ^{87}Rb vapor cell

Alkali vapor cell is the most critical part of CSAC, and its miniaturization is very significant yet challenging. Figure 2 shows the structure of the ^{87}Rb vapor cell with dual-chamber. One chamber serves as a reservoir and the other is the ^{87}Rb vapor chamber. The two chambers are connected with a very shallow channel. With the shallow channel, the generated ^{87}Rb vapor can diffuse to the left chamber in Fig. 2 to bring about light–atom interaction and the impurity generated in the reaction is on the left in the reservoir.

The fabrication procedure is schematically shown in Fig. 3. At first a shallow channel was fabricated on a silicon wafer by wet etching (Fig. 3(a)). Then two films of Si_3N_4 and SiO_2 were deposited on the silicon wafer successively by LPCVD technology (Fig. 3(b)). The etching window was patterned on both sides of the wafer by photolithography and wet etching (Fig. 3(c)). KOH etching solution was then put into the wafer for about 80 hours until the whole wafer was etched through. After that, a Pyrex glass plate was bonded to the silicon wafer to gain a bonded pre-form (Fig. 3(d)). ^{87}RbCl

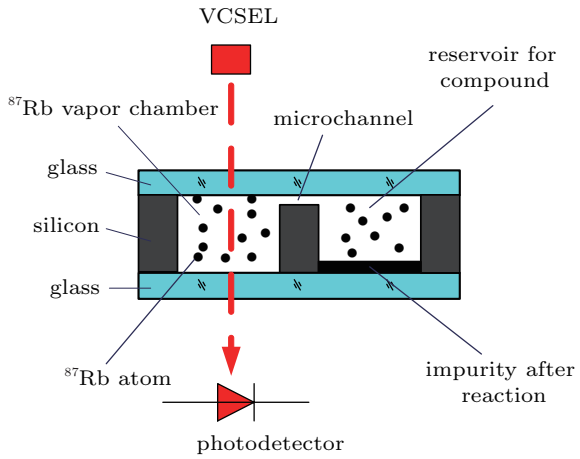


Fig. 2. (color online) Structure of the ^{87}Rb vapor cell with dual-chamber.

and BaN_6 were put into the reservoir with a transfer pipette (Fig. 3(e)). Finally, another Pyrex glass plate was bonded to the pre-form to obtain the ^{87}Rb vapor cell in the bonding machine (Fig. 3(f)).

During the bonding process, the chamber of bonding machine was pumped into high vacuum (below 3.0×10^{-6} mBar)

at first. The wafer was then heated to 200 °C and kept for an hour to let BaN_6 fully decompose into Ba and N_2. The generated N_2 was pumped out along with the decomposition. After the decomposition process, the chamber was filled by buffer gas and kept at 300 mBar for about 10 minutes, followed by covering the wafer with another Pyrex glass plate. The wafer was then heated to 300 °C rapidly, and a 1200 N force and 800 V voltage were applied on the Pyrex glass plate to complete anodic bonding. The bounded wafer was then kept at 300 °C for 30 minutes for full chemical reaction.

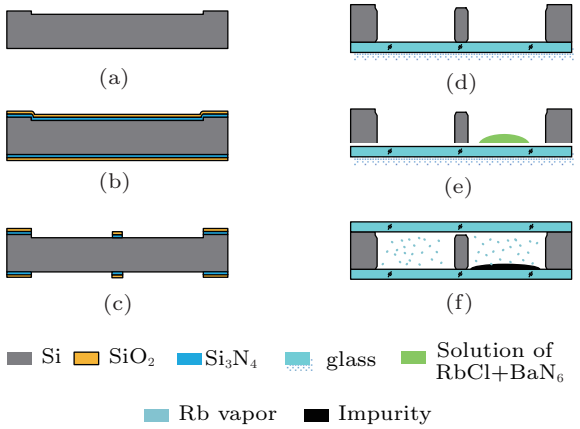


Fig. 3. (color online) Fabrication process of ^{87}Rb vapor cell. (a) Wet etching, (b) Si_3N_4 and SiO_2 thin film deposition by LPCVD, (c) mask patterned by wet etching, (d) KOH etching and anodic bonding, (e) dropping the solution of RbCl and BaN_6 into the reservoir of compound, and (f) anodic bonding to obtain ^{87}Rb vapor cell.

Figure 4(a) shows the wafer before dicing and figure 4(b) is the picture of one cell compared with a glass blowing ^{87}Rb bulb. The volume of the cell is 4.8 mm^3, two orders of magnitude smaller than the bulb made by a traditional glass blowing method.

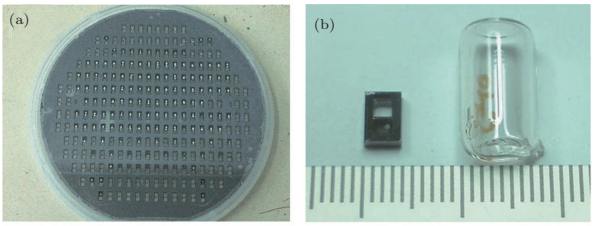


Fig. 4. (color online) Photograph of ^{87}Rb vapor cells. (a) Wafer of ^{87}Rb vapor cell, and (b) a ^{87}Rb vapor cell and a glass blowing ^{87}Rb bulb.

3. Integration of the physics package

As shown in Fig. 5, a vertical-integrated structure is adopted for the physics package. All the discrete components are integrated in a cuboid metal package made of kovar alloy. The physics package is connected to the servo circuit system through the pins of metal package for electrical interconnection.

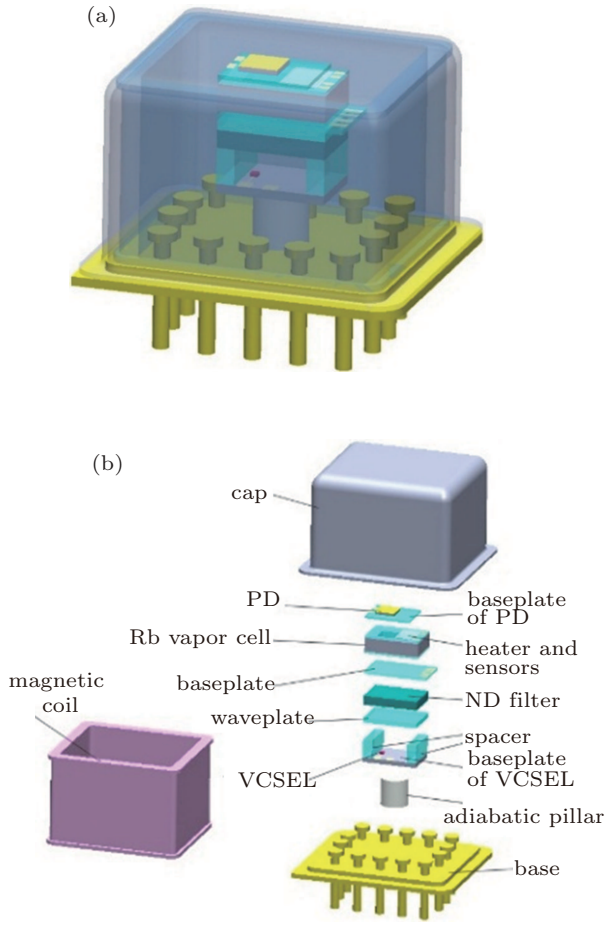


Fig. 5. (color online) (a) Schematic diagrams of the physics package of the CSAC. (b) Explored view.

3.1. Optical path design

The optical path of the physics package is shown in Fig. 6. The laser beam is emitted by a VCSEL placed on a silicon baseplate by flip-chip bonding. The laser beam passes through a $\lambda/4$ wave plate, an ND filter, and the ^{87}Rb vapor cell successively. Two glass spacers were mounted between baseplate of VCSEL and $\lambda/4$ wave plate in order to broaden the laser beam. Then the laser beam passed through the ^{87}Rb vapor cell and was monitored by a PD. The PD was placed on a glass baseplate by flip-chip bonding as well. Leading electrode pads were fabricated on the glass baseplate in advance. All these components were stacked up (Fig. 6) and assembled with an optical cement whose light transmittance could be as high as 80%.

The picture of baseplates of the VCSEL and PD is shown in Fig. 7. Pt thermistor and electrode pads were fabricated on the baseplate of the VCSEL. The VCSEL was placed on the pad and the PD was placed in the marked area among the four electrode pads.

3.2. Thermal management

Given that a Rb vapor cell should be maintained above 80 °C to ensure enough alkali atom density, heater and

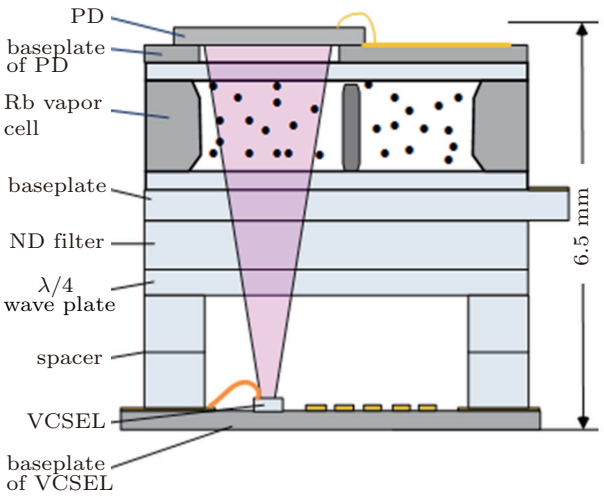


Fig. 6. (color online) Schematic diagrams of the optical path.

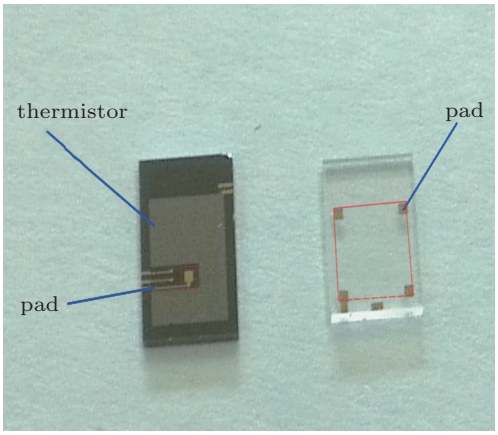


Fig. 7. (color online) Baseplates of the VCSEL and the PD.

thermistors are needed to control the temperature of Rb vapor cell precisely. The physics package of the NIST placed two planar heater structures made from a film of indium-tin oxide (ITO) deposited on a thin glass substrate on both sides of the Cs vapor cell to heat the cell to 85 °C to increase the Cs density correspondingly.[3] As shown in Fig. 8(e), Pt metal film was deposited on the glass surface to fabricate heater and thermistor which cover the reservoir, while the window of light–atom interaction chamber was left transparent. The temperature coefficient of resistance (TCR) of the Pt metal is much larger than ITO and the integrated heater and thermistors are closer to the temperature-control areas. Thus, the integrated heaters and thermistors have shown a better performance in precision of temperature control.

The heater and thermistor of Pt were fabricated by using a lift-off technology. Firstly, photoresist was patterned on the surface of wafer of Rb vapor cell by photolithography process, as shown in Fig. 8(a). Then Pt metal was deposited on the patterned photoresist using magnetron sputter, and a thin titanium (Ti) film was deposited before Pt in order to improve the adhesion between Pt and the substrate, as shown in Fig. 8(b). After that, the wafer of Rb vapor cell was soaked in acetone solution to totally remove the photoresist, as well as the Ti/Pt metal on the photoresist as shown in Fig. 8(c). At last, Au electrode pads for wire bond were fabricated, and the heater and thermistor were finally fabricated on the vapor cell, as shown in Fig. 8(d). The picture of heater and thermistor is shown in Fig. 8(e). The resistance of heater is about 100 Ω and the resistance of thermistor is about 12 kΩ at room temperature. The fabrication process of Pt resistances on the baseplate of VCSEL and the glass plate under ^{87}Rb vapor cell is the same as the process described above.

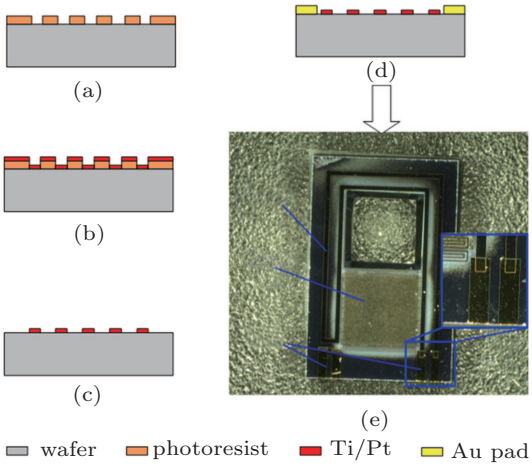


Fig. 8. (color online) Schematic illustration of heater and temperature sensor fabrication procedures. (a) Photolithography; (b) sputtering Ti/Pt; (c) photoresist stripping; (d) Au pad patterning; and (e) the picture of heater and sensor fabricated.

In order to reduce the power dissipation of thermal conductivity, a pillar made of polytetrafluoroethylene (PTFE) was used for the components stacking up, which was fixed on the base of metal package as shown in Fig. 5. Since the coefficient of thermal conductivity of the PTFE is very low (∼0.24 W/(m·K)), the temperature gradient of the whole system is mainly concentrated on the PTFE pillar and the temperature of metal package could be maintained at nearly room temperature. The power dissipation of PTFE-pillar-support-structure is higher than the suspension structure made of polyimide (PI), but it is much easier to fabricate and has better mechanical performance than the suspension structure made of PI. Meanwhile, the power dissipation of convection could be reduced by vacuum package. The power dissipation of the physics package is about 150 mW when the ^{87}Rb vapor cell is heated to 100 °C. The power dissipation could be further reduced by optimizing the size of PTFE pillar and the vacuum packaging of the physics package.

3.3. Magnetic coil and magnetic shielding

A magnetic coil was arranged outside the integrated stack of Fig. 6 to generate a weak magnetic field which defines the quantization axis and selects out the ^{87}Rb ground state $m_F = 0$

states for the CPT resonance. A cuboid metal package made of KOVAR alloy was used to cover the stack and magnetic coil for shielding vapor cell from the environmental electromagnetic fields. A demagnetization process was used before the metal package was sealed. The electrode pads of the VCSEL, PD, heater, thermistor, and magnetic coil were connected to the pins of the metal package by wire bond. At last, the physics package could be vacuum-sealed in vacuum encapsulation system to reduce the power dissipation of convection. The picture of physics package of chip-scale atomic clock is shown in Fig. 9. The total volume of physics package is about 2.8 cm^3.

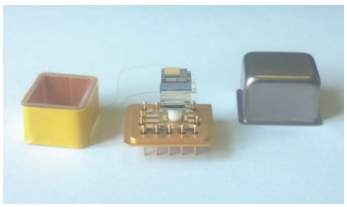


Fig. 9. (color online) Picture of physics package for the CSAC.

4. Experimental results

4.1. Optical absorption spectrum

With the physics package, the optical absorption spectrum has been recorded. Through the driving current, the frequency of the VCSEL output laser was repeatedly scanned around the D1 transitions of ^{87}Rb, the temperature of the vapor cell was slowly increased, and transmitted spectrum was detected with a PD, as shown in Fig. 1. When the temperature reached 75 °C, clear absorption lines were observed. Figure 10 shows the absorption spectrum recorded when the temperature was at 100 °C.

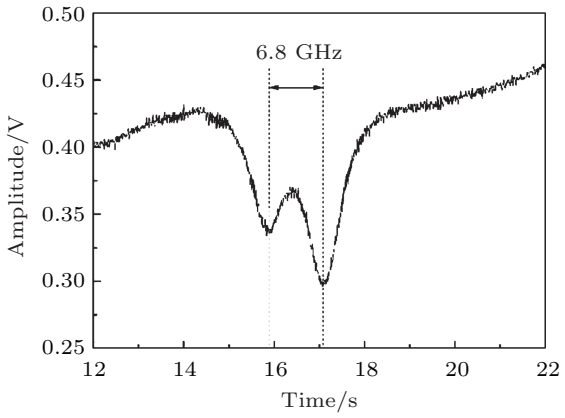


Fig. 10. Optical absorption spectrum of ^{87}Rb vapor cell at 100 °C.

4.2. Microwave frequency correction signal

In order to obtain microwave frequency correction signal, the driving current of the VCSEL has been modulated with $\nu/2 \approx 3.4$ GHz (the half of ^{87}Rb ground state hyperfine splitting), so that it outputs FM multi-chromatic laser and the ± 1 sidebands were used as bi-chromatic laser to CPT resonant with atoms. From the signal detected by PD, narrow line width CPT signal will be extracted as microwave frequency discriminating signal and be converted into frequency correction signal to lock the output frequency of the atomic clock. Figure 11 presents the microwave frequency correction signal obtained with the physics package. It indicates that the fabricated physics package can meet the application requirements of the CSAC.

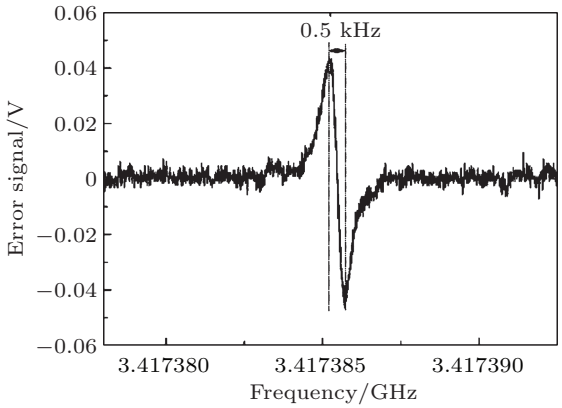


Fig. 11. Microwave frequency correction signal obtained with the physics package.

4.3. Frequency stability of the CSACs

The physics package of the CSAC has been experimentally tested by connecting with laboratory electronics equipment to form a table top atomic clock, and the short-term frequency shown in Fig. 12 has been measured when the vapor cell was heated to 100 °C and VCSEL was maintained at 85 °C. It is seen that within 100 s Allen deviation displays the $\tau^{-1/2}$ behavior characteristic of atomic clock[8] and the short-term frequency stability is about $7 \times 10^{-10}\tau^{-1/2}$. The physics package has not been vacuum-sealed yet, and the power dissipation is 150 mW, a little high for a chip-scale application. However, it will not be difficult to improve with the aid of experience of the achieved one.

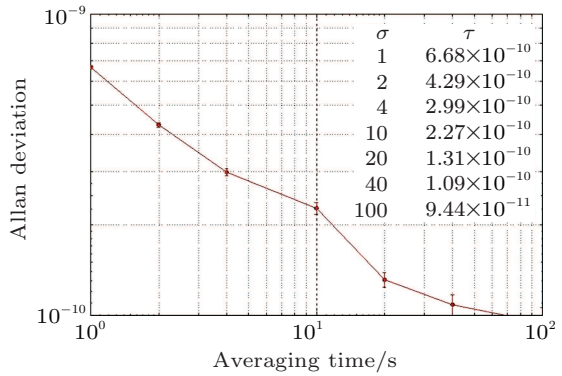


Fig. 12. (color online) Short-term frequency measured with the CSAC physics package.

5. Conclusion

An integrated physics package of the CSAC was successfully developed. All the discrete components were integrated into a cuboid metal package with a volume of about 2.8 cm^3. In the physics package, Rb vapor cell was batch-fabricated based on the MEMS process technology and *in-situ* chemical reaction method. Pt heater and thermistors were integrated in the physics package and the optical elements in the physics package were supported by a PTFE pillar to reduce the power dissipation. By connecting the physics package with the servo circuit system, the microwave frequency correction signal was obtained, thus a CSAC was finally realized with the physics package. In the experiment, the short-term stability of $7 \times 10^{-10}\tau^{-1/2}$ was achieved when the ^{87}Rb vapor cell was heated to 100 °C and the temperature of VCSEL was maintained at 85 °C. All the results prove that the successfully fabricated physics package meets the requirement of the CSAC. Because the physics package was not vacuum-sealed yet, the power dissipation is a little high (∼150 mW) and temperature control accuracy is not good enough. For the next step we could seal the physics package in vacuum packaging equipment to further improve the performance of the physics package of CSAC.

Acknowledgment

The authors gratefully thank Gu Sihong, Zhang Yi, Yang Jing, and Tian Yuan at Wuhan Institute of Physics and Mathematics, Chinese Academy of Science for valuable technical discussion and the testing work.

References

[1] Lutwak R, Emmons D, Riley W and Garvey R M 2002 34*th Annual Precise Time and Time Interval (PTTI) Meeting*, Reston, Virginia, p. 539

[2] Liew L, Knappe S, Moreland J, Robinson H, Hollberg L and Kitching J 2004 *Appl. Phys. Lett.* **84** 2694

[3] Knappe S, Shah V, Schwindt P D D, Hollberg L and Kitching J 2004 *Appl. Phys. Lett.* **85** 1460

[4] Gerginov V, Knappe S, Schwindt P D D, Shah V, Liew L, Moreland J, Robinson H G, Hollberg L, Kitching J, Brannon A, Breitbarth J and Popovic Z 2005 2005 *IEEE International Frequency Control Symposium and Exhibition*, Vancouver, Canada, p. 758

[5] Knappe S, Schwindt P D D, Shah V, Hollberg L, Kitching J, Liew L and Moreland J 2005 *Opt. Express* **13** 1249

[6] Lutwak R, Deng J, Riley W, Varghese M, Leblanc J, Tepolt G, Mescher M, Serkland D K, Geib K M and Peake G M 2004 36*th Annual Precise Time and Time Interval (PTTI) Meeting*, Washington DC, USA, p. 339

[7] Mescher M, Lutwak R and Varghese M 2005 *The Draper Technology Digest* **10** 26

[8] Lutwak R, Vlitas P, Varghese M, Mescher M, Serkland D K and Peake G M 2005 *IEEE International Frequency Control Symposium and Exhibition*, Vancouver, Canada, p. 752

[9] Knapkiewicz P, Dziuban J, Walczak R, Mauri L, Dziuban P and Gorecki C 2010 *Procedia Engineering of Eurosensors Conference*, Linz, Austria, p. 721

[10] Vecchio F, Venkatraman V, Shea H, Maeder T and Ryser P 2010 *Procedia Engineering of Eurosensors Conference*, Linz, Austria, p. 367

[11] Straessle R, Pellaton M, Affolderbach C, Petremandet Y, Briand D and Mileti G 2013 *J. Appl. Phys.* **113** 064501

[12] Su J, Deng K, Guo D Z, Wang Z, Chen J, Zhang G M and Chen X Z 2010 *Chin. Phys. B* **19** 110701

[13] Liu Z, Wang J Y, Diao W T, He J and Wang J M 2013 *Chin. Phys. B* **22** 043201

[14] Xu Z X, Qu W Z, Gao R, Hu X H and Xiao Y H 2013 *Chin. Phys. B* **22** 033202